

Novel Authentic and Ultrafast Organic Photorecorders Enhanced by AIE-Active Polymer Electrets via Interlayer Charge Recombination

Chun-Yao Ke, Mei-Nung Chen, Mu-Huai Chen, Yen-Ting Li, Yu-Cheng Chiu,*
and Guey-Sheng Liou*

Organic photonic memory, featuring a variety of glamorously light-driven characteristics, is rapidly growing into an indispensable building block for next-generation optical communication systems. However, the ambiguity of their operating mechanism associated with the limitation of photoadaptive materials as an electronics promoter results in the slow development of photonic transistor-based devices. In this study, the conjugated polymers composed of donor–acceptor motifs with typical aggregation-induced emission (AIE) behaviors are designed and successfully discover high-performance photoprogrammable memory. Moreover, the mechanism of photoboosted recording behavior, attributed to the recombination of the formed interlayer excitons right after simultaneous excitation without applying vertical and parallel electric-field at the interface in-between active semiconductor and AIE polymers, is cautiously corroborated by steady-state PL and pulse PL measurements. The AIE-polymer memory devices perform ultrafast photoresponse time of 0.1 ms, an outstanding current switch ratio up to 10^6 , and retention stability over 40 000 s without significant dissipation. Furthermore, photoresponsive AIE-polymer electrets not only modulate the memory performance through the emission wavelength but easily switch storage behavior of nonvolatile memory from flash to WORM by adjusting the torsion-angle through the motif of the donor and acceptor moieties. These findings open an avenue for designing conjugated polymer electret for ultrafast optical storage devices.

1. Introduction

Following the explosive growth of information and the rapid evolution of computing speed, the technology of optical-communication systems^[1] featuring high security, high speed, low latency, and low interference characteristics have been urgently desired in various application of artificial synaptic memory,^[2] encrypted storage,^[3] wearable sensorimotor,^[4] and nonvolatile flash memory.^[5] Compared with conventional electric-driven memory, the novel photo-modulated memory has arisen enthusiasm of researchers because of their energy-saving, ultrafast transmission, and orthogonal operability in voltage stress as well as optical pulse. These outstanding potentials comfortably resolve the bottleneck of significant delays regarding von Neumann architecture unstructured data analysis, processing of large images, and field of artificial intelligence.^[6] However, the progress of this crucial topic, up to date, is far behind voltage-driven nonvolatile memory, blaming on the lack of comprehensive commentary that could precisely provide the criteria for the design of photo-


adaptive materials and the pattern for the configuration of photonic FET memory device.

Recently, several approaches to photoprogramming behavior through the blending semiconductor structure and floating gate systems have been reported in the field of OFET memory. The blending system by mixing inorganic perovskite quantum dot, n-type polymer, and photochromic materials in the p-type semiconductors, could simply manufacturing process and store charge in the valley of energy-level.^[7] However, this approach may bring about an adverse impact on semiconducting performance. Besides, photoactive materials such as lanthanide and perovskite are utilized as charge storage sites in floating gate architecture.^[8] These photoluminescent (PL) materials as the memory layer inhere prominent behavior since the emitted light could be further absorbed by the semiconductor layer upon photoexcitation that produces the electron–hole pairs and

C.-Y. Ke, M.-H. Chen, Prof. G.-S. Liou
Institute of Polymer Science and Engineering
National Taiwan University
No.1, Sec. 4, Roosevelt Road, Taipei 10617, Taiwan
E-mail: gsliou@ntu.edu.tw

M.-N. Chen, Y.-T. Li, Prof. Y.-C. Chiu
Department of Chemical Engineering
National Taiwan University of Science and Technology
No.43, Sec. 4, Keelung Rd., Da'an Dist., Taipei City 10607, Taiwan
E-mail: ycchiu@mail.ntust.edu.tw

Prof. Y.-C. Chiu, Prof. G.-S. Liou
Advanced Research Center for Green Materials Science and Technology
National Taiwan University
Taipei 10617, Taiwan

 The ORCID identification number(s) for the author(s) of this article can be found under <https://doi.org/10.1002/adfm.202101288>.

DOI: 10.1002/adfm.202101288

subsequently separates by external bias to be captured in the specific trapping sites.^[9] Therefore, if their emissive wavelength and the absorbance of the employed semiconductor can match smoothly, the performance of memory devices is expected to be improved significantly. To shorten the photoprogramming time, the recently reported photoinduced memories utilized luminescent inorganic materials wrapped in insulating polymers to create specific morphology of inorganic materials for greater contact area in-between the semiconductor and charge-storage layer.^[10] Unfortunately, those strategies are not appreciated for large-area production, which necessarily considers the blending ratio, dispersion of photoresponsive substances, and specific morphology.

In our previous study, the conjugated donor-acceptor polymers, poly(triphenylamine)s (PTPAs), as plenary-contact area materials incorporating distinctive luminescent characteristics by introducing different acceptor groups to precisely dominate the luminescence behavior, corresponding emission wavelength, and even the energy-level, can become excellent candidates for the application to photonic memory or photorecorder.^[11] Among the PTPAs, PTPA-CN and PTPA-CNBr featuring specific functional groups (cyano, α -cyano-stilbene) in the sidechain of triphenylamine-core possess AIE-behavior emitting forceful blue and orange light, respectively, and also exhibit admirable capability of hole trapping in voltage-driven memory.^[12] Nevertheless, the PTPA-3CN with pendant group of tricyano-vinyl inhering the strongest electron-withdrawing ability in PTPAs, which displays nonluminous aggregation-caused quenching (ACQ) behavior owing to the highly planar structure and formidable intramolecular charge-transfer, could exactly capture two kinds of polar carriers under voltage-driven operation.

Herein, novel photoprogrammable nonvolatile transistor memory devices with easily solution-processable AIE-polymer electrets and, importantly, their corresponding mechanism are demonstrated. The prepared photoinduced memory devices with AIE-polymers manifest ultrafast photoresponse in 0.1 ms, high current switch ratio up to 10^6 , and the retention stability over 40 000 s without significant dissipation. To the best of our knowledge, this is the fastest organic photonic transistor memory up to date. Through steady-state PL and pulse-PL analyses, we could directly observe the formation of interlayer exciton within vertically stacked semiconductor/AIE-polymers, where the semiconductor supplies the electrons while the electret material provides the holes, thereby forming the authentic photoprogramming memory. Namely, a realization of the optical-writing phenomenon only requires the dual-layer excitation instead of supplying vertical electric fields required in conventional transistor memory. On the contrary, even the optical stimulus with long exposure time, the device derived from the nonfluoresced PTPA-3CN as electret with mismatched energy-level to the semiconductor resulted in no output-current signals for light recording. In short, herein the novel and innovative investigation of conjugated AIE polymers create both photoadaptive capability and ultrafast response for the photonic transistor memory. This discovery is a key to design high-performance photoactive electrets for light recorders and provides energy-saving operating patterns in transistor-based memory systems.

2. Results and Discussion

2.1. P-Type Photonic Memory Employing PTPAs Based Electret

The configuration of a photoprogrammable transistor memory device based on typical bottom-gate (BG) and top-contact (TC) OFET is illustrated in Figure 1a. The PTPA derivatives with varied photoluminescence behaviors were spin-cast on the top of SiO₂/Si⁺⁺ substrates. Pentacene as a p-type transporting layer was deposited on the top of studied polymer electrets by thermal evaporation. Through the PL information of PTPAs shown in Figure S1 (Supporting Information), PTPA-CN and PTPA-CNBr reveal conspicuous emission peaks at 457 nm (blue light) and 576 nm (orange light), respectively. On the contrary, PTPA-3CN with a strong electron-affinity group (tricyano-vinyl) performs intra- and intermolecular charge transfer, indicating that PTPA-3CN is ACQ-polymer. As a result, the introduced functional groups (cyano or α -cyano-stilbene) into PTPA-CN and PTPA-CNBr behaving AIE phenomena demonstrate that could allow the light-excited excitons to consume energy through the luminescent emission. The detailed synthetic preparation, fundamental thermal, optical, and electrochemical properties of monomers and polymers have been attentively discussed in our previous literature.^[11]

To explore the photostorage characteristics of the PTPAs memory devices, the red-green-blue (RGB) light was utilized as the stimulating source without gate and source-drain voltage applied in neutral devices in Figure 1b–d. The results manifest the hole-transporting behaviors of the transfer curve as previous report^[13] with an on/off current ratio of 10^3 . The PTPA-CN- and PTPA-CNBr-based devices exhibited distinctly positive shifted threshold voltage (the programmed state) after the appropriately illuminated operation. The changed onset of transfer curves could present the information of electret materials, including the capability of storage and polarity of charges. As a result, AIE-polymer devices demonstrated the behavior of photoinduced charge-trapping under blue-light, while the PTPA-CNBr-based device could also respond under green-light in addition to blue-light. However, the transfer curve of AIE-polymer devices revealed no noticeable shift under red-light. Our findings confirm that the photoboosted behaviors tightly correspond with the UV-vis absorption of two electret layers as shown in Figure 1e,f, respectively. It is worth mentioning that PTPA-CN- and PTPA-CNBr-based devices under voltage-driven operation exhibit hole-trapping only. (Figure S2, Supporting Information). Interestingly, the PTPA-3CN, an ambipolar electret material with the ability to capture two different polarities of charges in pentacene-based memory devices (Figure S2, Supporting Information), possesses the widest absorption range and the most significant photosensitivity among all PTPAs (Figure 1g). However, the operating transfer curve of the PTPA-3CN-based device in Figure 1d still maintains the same trace as the initial curve, despite elongating the exposure time of RGB light sources to 2 min, as shown in Figure S3 in the Supporting Information. This unexpected phenomenon reveals that the working principle of memory between voltage-driven and optical-driven is entirely different. As a result, the target AIE-polymers in this work open the photoinduced memory behavior for the configuration of transistor-type memory devices, where the actuation light is closely related to the absorption nature of the AIE-polymers. In strong contrast to

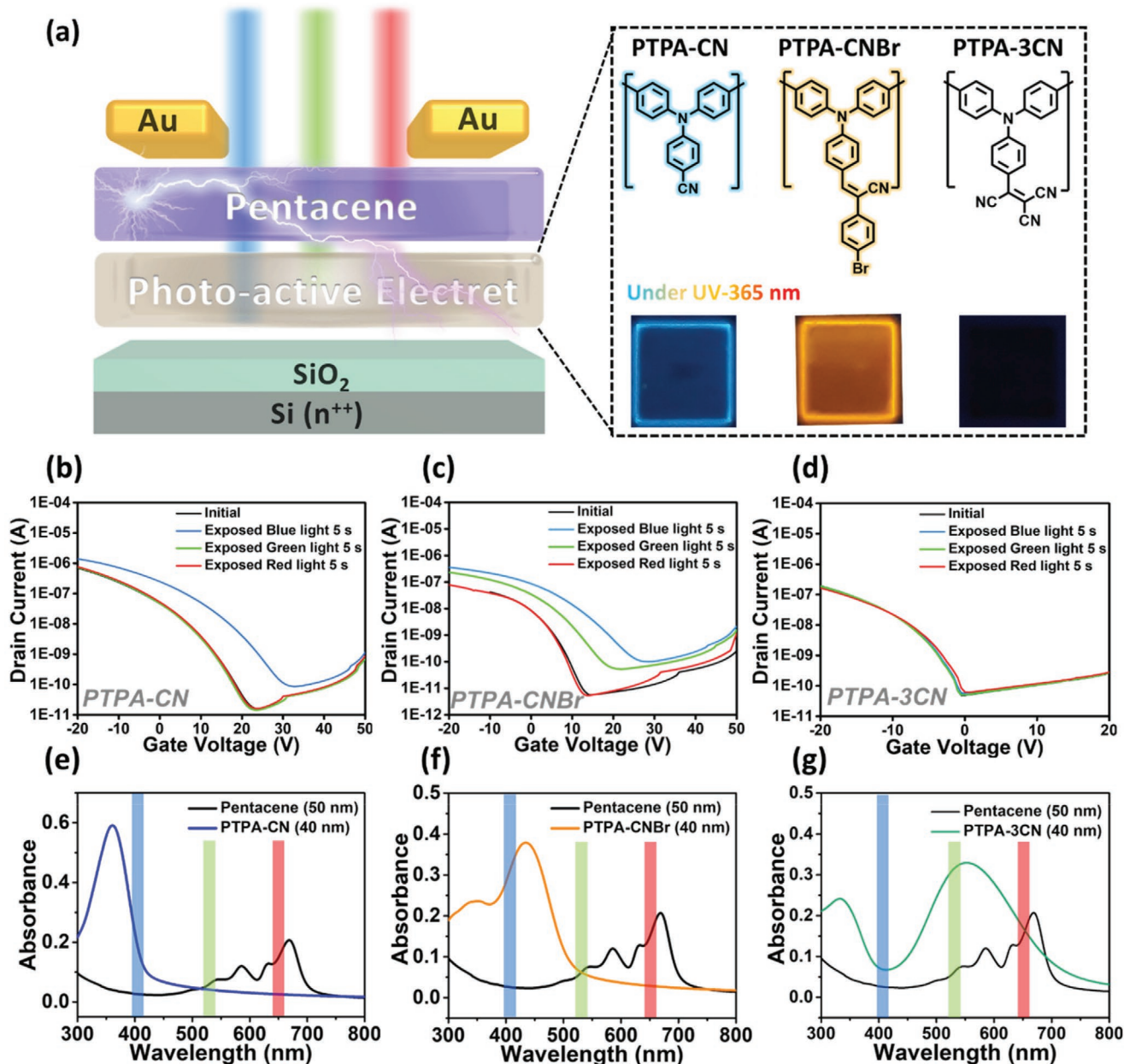


Figure 1. a) Schematic illustrations of the studied photoprogrammable recorder device, relevant molecular structures, and luminescence characteristics. b–g) Transfer characteristics of the photoprogramming states with corresponding UV–vis absorption spectra of b,e) PTPA-CN, c,f) PTPA-CNBr, and d,g) PTPA-3CN. The devices were exposed to the fixed light intensity (5 mW) with different wavelengths for 5 s photoprogramming operation, and the transfer curves were measured after 3 min. All currents were measured at the fixed drain voltage ($V_{DS} = -60$ V) in the truly dark. (blue light: 395–415 nm; green light: 522–542 nm; red light: 640–660 nm).

AIE polymers, the studied ACQ polymer suppresses the photoresponse effect even though the corresponding device did have the electron-trapping capability through a voltage-driven operation.

2.2. Observation of Interlayer Charge Recombination in Double-Layer Heterostructures with PTPAs

To further investigate the relationship between the emissive behavior of AIE-polymers and the photoprogramming

performance in these devices, the steady-state PL measurement of single-layer with pure AIE-polymers and double-layer with the deposited pentacene on the polymers were measured and illustrated in Figure 2a,b. The PTPA-CN and PTPA-CNBr samples with unilayer (dash-line) and bi-layer (solid-line) structures were excited by 405-nm light, exhibiting emission peaks at 457 and 576 nm, respectively. Afterward, compared with the emission intensity of unilayer film on quartz, that of bilayer is dramatically decreased by 63% (PTPA-CN) and 73% (PTPA-CNBr), respectively. The results of conspicuously PL intensity

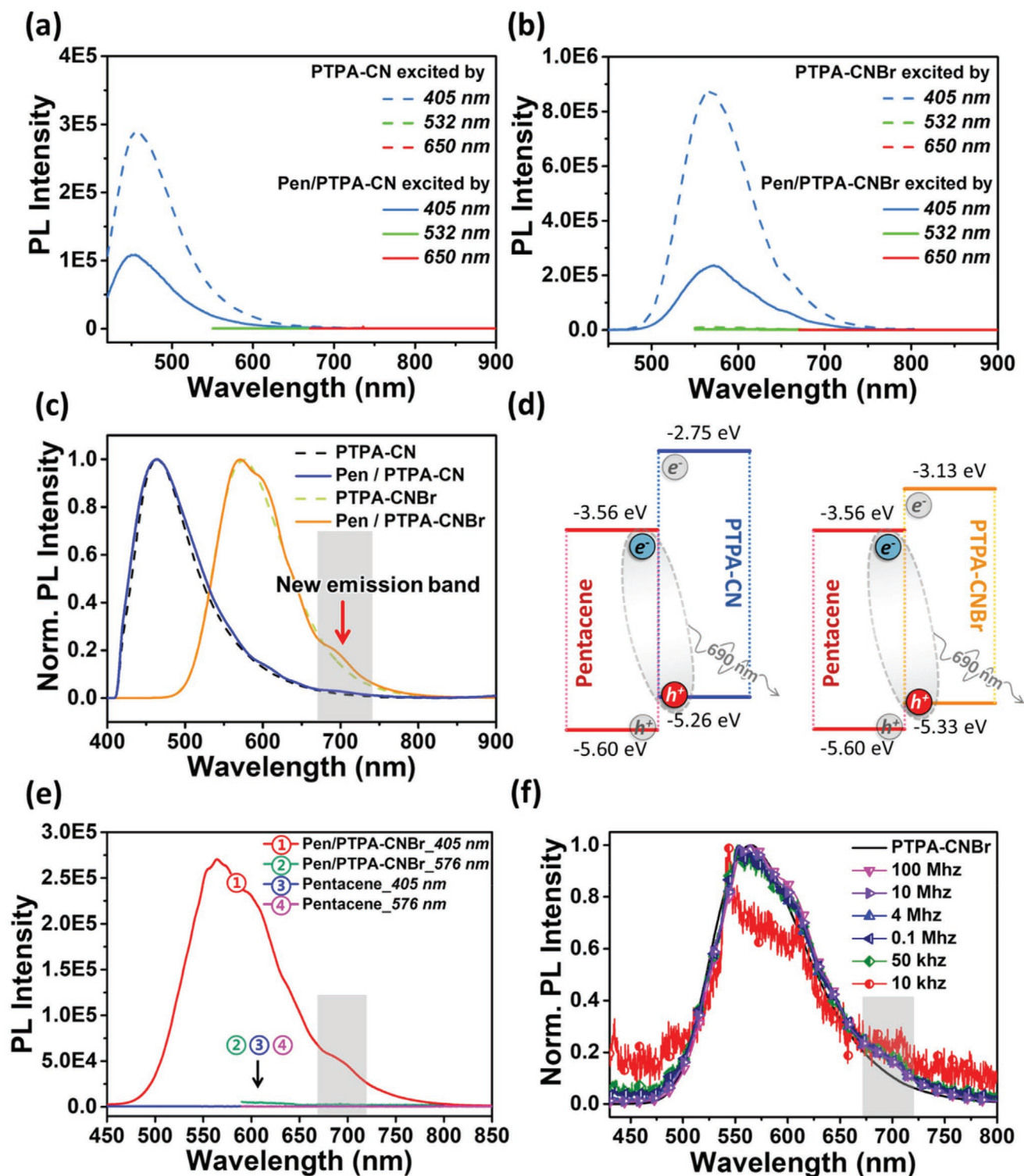


Figure 2. Steady-state PL spectra of a) PTPA-CN (dash line), pentacene/PTPA-CN bilayer (solid line), and b) PTPA-CNBr (dash line), pentacene/PTPA-CNBr bilayer (solid line) with excitation wavelength from 405 to 650 nm. c) Normalized PL spectra of unilayer AIE-polymers and bilayer structure composed of pentacene and AIE-polymers. The new emission band near 1.78 eV indicates the formation of interlayer excitons. ($\lambda_{\text{ex}} = 405 \text{ nm}$) d) Illustration of the band alignment of pentacene/PTPA-CN and pentacene/PTPA-CNBr bilayer. Photoexcitation of the pentacene/PTPA-CN and pentacene/PTPA-CNBr bilayer leads to tightly bound interlayer excitons, with electrons (e^-) in pentacene and holes (h^+) in AIE-polymer. e) The PL spectra of bilayer and single pentacene structure excited by 405 and 576 nm. f) Normalized Pulsed-PL spectra with pentacene/PTPA-CNBr bilayer structures utilized diverse incident pump frequencies from 10 kHz to 100 MHz, and the duration time is 60 ps.

quenching could be regarded as evidence of the efficient energy transfer between AIE-polymers and pentacene.^[8a] Inspection of the normalized PL spectra (Figure 2c) with 405-nm photoexcitation on pentacene/AIE-polymer devices shows that an additional low-energy emission peak near 690 nm (1.78 eV) could be observed apart from the original peaks of polymers. However, the PL spectra of PTPA-3CN deposited with pentacene did not reveal the additional emission peak under excitation wavelength ranging from 405 to 650 nm as shown in Figure S4 in the Supporting Information. All the pentacene/AIE-polymers bilayer-structure samples present the additional low-energy emission peak, and the hypothesis regarding the additional emission band is suggested through an energy-level diagram in Figure 2d. The difference of the highest occupied molecular orbital (HOMO) levels for PTPA-CN/PTPA-CNBr (−5.26/−5.33 eV) and pentacene (−5.60 eV) is higher than 0.15 eV which is the pentacene binding energy of Frenkel excitons.^[14] The appropriate energy level facilitates a higher possibility of the relaxation pathway for photogenerated excitons. Therefore, the noticeably additional emission band with the bandgap of 1.78 eV could be attributed to interlayer-recombined exciton from the lowest unoccupied molecular orbital (LUMO) of pentacene and the HOMO of the AIE-polymers.^[15] In contrast, the HOMO level between PTPA-3CN (−5.51 eV) and pentacene is too close to provide sufficient driving force for surmounting the Coulombic interaction of bound excitons generated in pentacene, as shown in Figure S5 in the Supporting Information. Hence, the PTPA-3CN-based device, behaving with unique voltage-driven memory properties, is unable to convert the optical stimulus into the electrical signals through the interlayer excitons between PTPA-3CN and pentacene. Based on the energy-band alignment and normalized PL spectra, we have affirmed the requirement of an energy level match between AIE-polymers and pentacene. It is noted that devices with various thicknesses of pentacene have been investigated and performed similar capability of trapping electron (Figure S6, Supporting Information), indicating that the interlayer-exciton is not dependent on the thickness of pentacene and likely to generate only at the interface between electret and pentacene. The recombination of interlayer excitons is spontaneously succeeded, in which the electrons are supplied from the pentacene and the holes provided from the AIE-polymers. Thus, it is an indispensably crucial issue that the semiconductor and photoactive electret layers must be excited simultaneously to generate excitons under an exposed environment for realizing that the luminescence electrets could effectively enhance the photoprogramming behavior.

2.3. Occurrence and Dynamic Procedure of Interlayer Exciton

To soundly corroborate that the existence of interlayer charge recombination could occur solely under the dual-layer exciting circumstance, the intentionally designed experiments were carried out using PTPA-CNBr as the photoactive layer in the following measurements to support our proposed mechanism. As shown in Figure 2e, the excitation source at 576 nm, the same as the emission wavelength of PTPA-CNBr, was selected to mimic the situation of the top pentacene layer illuminated by

the orange light from the polymer electret. In other words, the excitons only subsist in the upper pentacene excited by 576 nm light for the bilayer architecture. Compared with curve 1 excited by 405-nm light in Figure 2e, curve 2 displayed the nonluminescent behavior of PTPA-CNBr under 576 nm photoexcitation and revealed no extra emission band from interlayer charge recombination. Moreover, the luminescent intensity of the additional emission band (Figure 2e, curve 1) is much stronger than that of pentacene (Figure 2e, curves 3,4), implying that pentacene as the source of interlayer exciton irradiation can be excluded.^[16]

To elucidate the results of AIE-polymers exhibiting dual-layer excitations demonstratively, the pulse-PL measurement with different pumping frequencies was employed to construct the details of the optical-modulating procedure. With increasing the pulsed frequencies, the luminescence intensity of AIE-polymer displays higher since the interval between each laser pulse becomes more compact. For example, the operating frequency of 10 kHz represents an interval of 0.1 ms, while 100 MHz is 10 ns, indicating that the sample could be triggered to generate more photoexcited excitons by densely photon-pumping within a constant period. Because the lifetime of a photoexcitation exciton for common organic materials is about 10^{-8} – 10^{-9} s,^[9b,17] Thus, the shortest interval pulse (100 MHz) was designated to timely supplement refreshing excitons into AIE electret by the subsequent pulse. Consequently, the excitons of pentacene induced by emissive AIE polymer could preserve to form interlayer charge recombination. In Figure 2f, the Pulse-PL measurement for the bilayer specimen consisting of PTPA-CNBr and pentacene using 405 nm pulse with 60 ps duration time was conducted at high pulse repetition rates of 10 kHz, 50 kHz, 100 kHz, 4 MHz, 10 MHz, and 100 MHz, respectively. Surprisingly, the results show that the interlayer charge recombination from interlayer excitons can be observed regardless of the operating frequency as shown in Figure S7 in the Supporting Information. In other words, even though the operational frequencies feature long intervals (10 kHz to 10 MHz), the consequences induced by each pulsed laser could be regarded as independent, and the additional emission peak could also be observed under individual irradiation with an excitation time of 60 ps. When the operating frequency increases, accordingly stronger light intensity at 690 nm could be obtained, which is attributed to the formation of the more concentrated interlayer excitons. Consequently, the action of photoprogramming caused by the interlayer exciton possesses possible potential to be accomplished in an ultrafast operating time.

2.4. Working Principle for “Photoinduced Memory” Behavior

Herein, we propose a plausible mechanism to interpret the photoprogrammable behavior comprehensively, as illustrated in Figure 3. The photoprogramming phenomenon for the pentacene-based transistor memory device with AIE-polymers as photoresponsive electret layer is composed of four successive progressions (using PTPA-CNBr as an example): (i) The photogenerated excitons accumulate within the bottom PTPA-CNBr layer upon exposing 405-nm light that provides the higher photon energy than energy bandgap (E_g) of the photoactive material

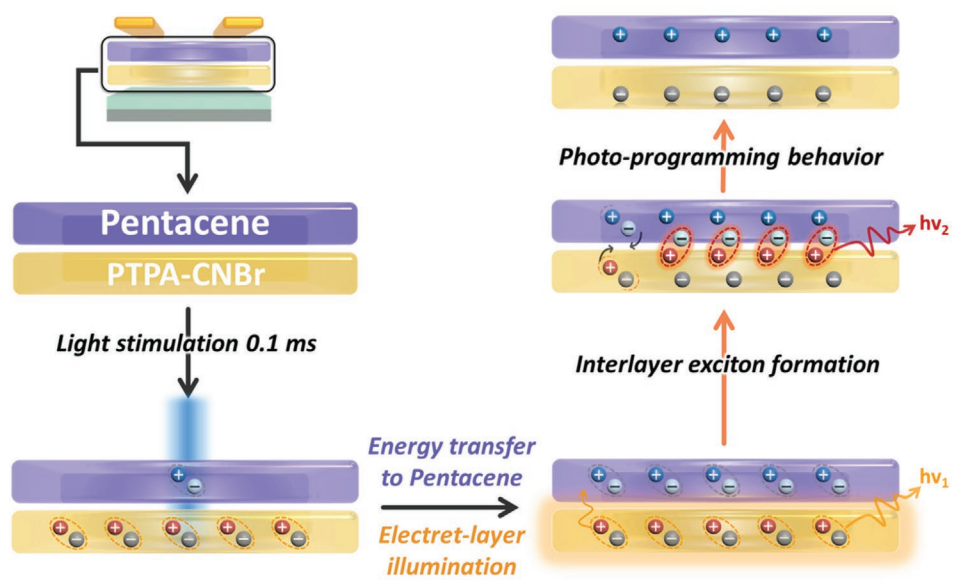


Figure 3. Schematic diagrams of the mechanism of photoprogramming under blue light illumination based on PTPA-CNBr electret memory device.

featuring sufficient absorption ability to the light stimulation. (ii) The fractional excitons generated in PTPA-CNBr would self-recombine and thus emit shiningly orange light. Then, the upper pentacene could effectively absorb the emitting light to produce excitons. In other words, the phototriggered excitons can exist simultaneously both in the two mutual-contact layers under incessant irradiation. (iii) According to the proper energy level alignment, a new additional emission band derived from interlayer excitons could also be observed at a more bathochromic position. (iv) Finally, electrons reside in the PTPA-CNBr layer and holes remain in pentacene. As a result, the mechanism of the photoprogramming process could be constructed.

2.5. Authentic Organic Photorecorder Enhanced by AIE-Active Polymer Electrets

The influence of emission wavelength from the targeted electret layer on the photonic memory device is presented in **Figure 4a,b**. The transfer curve would significantly shift to the positive direction after light exposure, resulting from the numerous electrons stored in the electret layer through yielding plenty of interlayer exciton recombination, which accomplishes and obtains the genuine photoprogramming behaviors. The process is similar to conventional transistor memory, utilizing external electrical stress to inject electrons into the charge storage layer. Moreover, the stability of the programmed photonic memory device was demonstrated to be valid as illustrated in **Figure 4c,d**. The transfer curve was scanned at 2, 12, 24, and 48 h after exposure to blue light, confirming that no significant change in the behavior of storage electrons (the vertical and parallel electric field was exempted within programming and resting period to achieve the definition as an authentic photonic memory). Besides, the retention tests at a reading gate voltage of 15 V confirm that the optical-writing information regarding current contrast and stability could be well preserved as shown in **Figure 4d**.

In **Figure S8** (Supporting Information), the results show that the photoinduced memory window of the PTPA-CNBr-based device can be boosted more pronouncedly than the case based on the PTPA-CN electret after lengthening the exposure time. Since the uninterrupted excitons are generated in the electret layer under external light stimulation, the optical-modulating performance should be dominated by the absorption of pentacene toward the emitted light of luminescence polymer electret. The emissive characteristic of AIE-polymers (40 nm) and the absorption of pentacene (50 nm), as depicted in **Figure S9** (Supporting Information), indicates that pentacene prefers to absorb the longer emission wavelength of PTPA-CNBr. Consequently, the orange light supplied from PTPA-CNBr should facilitate more effectively to generate the abundant excitons in the pentacene for enhancing the photoinduced memory window, even though that the energy barrier between PTPA-CN and pentacene is smaller than that of PTPA-CNBr.

It is worth mentioning that the inherent weakness of p-type semiconductor systems may be thought of as limited by the deficiency of minority carriers for charge trapping,^[18] resulting in tiny or invisible memory windows by voltage-driven operation even though the electret materials possess a powerful electron-affinity ability.^[19] In short, the sensational photoprogramming operation with luminescent polymer electrets where the photons could rapidly convert optical energy into photoexcited excitons for effectively enhancing the concentration of minority carriers to augment the memory windows. Furthermore, contrary to the most denounced problem of the voltage-driven operation (the electrical stresses are essential to inject charges), the optical-driven mechanism works very well without the application of vertical or parallel electric fields. The unique and peculiar behaviors demonstrate that this photoprogrammable process is not only energy-saving and environment-friendly but complements storage operations in ultrafast time. Put differently, the light as the fourth electrode can substitute for the gate electrode in a transistor-based configuration.

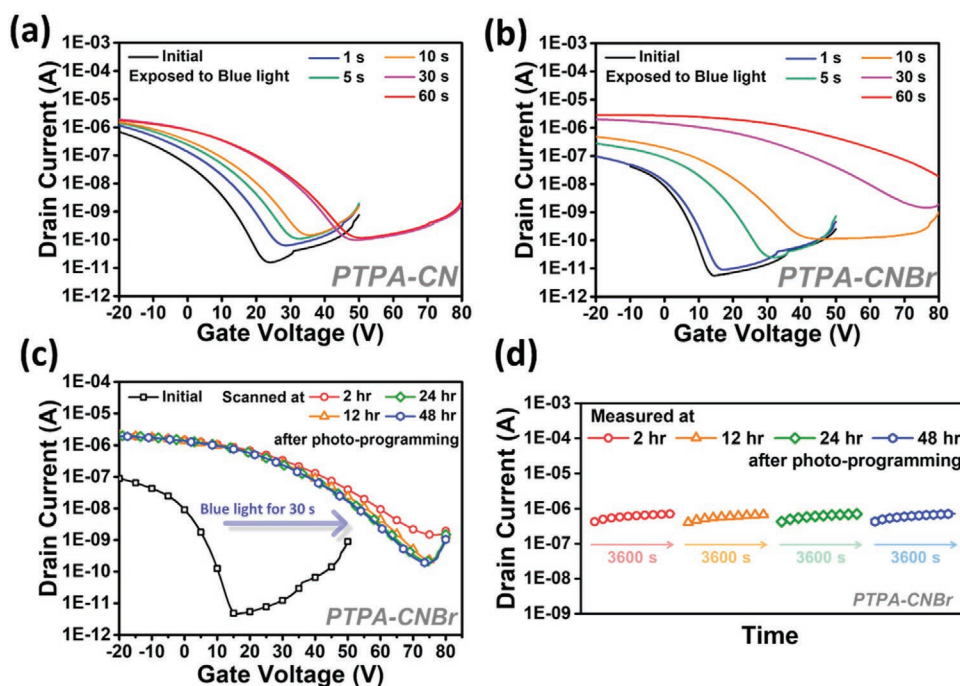


Figure 4. Presenting the transfer curve of a) PTPA-CN, b) PTPA-CNBr device under different irradiation time ranging from 1 to 60 s. The c) transfer and d) retention characteristics of authentic photonic memory with PTPA-CNBr electrets, these curves were preserved in a dark environment for 2, 12, and 48 h before scanning.

2.6. Ultrafast Responsive PhotoRecorder and Tunable Storage Behavior via AIE-Electret

To investigate the characteristic of light-writing for the versatile applications, two cardinal parameters, light-programming time and reversed-application voltage to the initial state, should be quantified through the in situ measurements including vertical or parallel electrical field effect. In Figure 5a,b, the temporal currents of initial curves maintain at a quite stable low conducting state (10^{-11} – 10^{-12} A) in the dark, implying that the applied electrical field has not deteriorated the original devices. By triggering blue light for 1–10 s on the working AIE-polymer-based memory devices, the source-drain currents abruptly bounce and are measured up to 10^{-6} A, afterward, obviously achieving on/off (high/low) current ratio of 10^5 and 10^6 (PTPA-CN and PTPA-CNBr) by scanning transfer curve after the in situ optical-writing procedures, as illustrated in the Figure S10 in the Supporting Information. Hence, the in situ operations could be used to determine the optimal illuminated-induced time for PTPA-CN and PTPA-CNBr with the photoprogramming feature, which is 5 and 1 s, respectively. In Figure 5c, the long-term retention measurement, a pivotal issue for examining charge storage stability as nonvolatile photoprogrammable memory devices, displays the remarkable steady I_{DS} for more than 40 000 s without significant dissipation. Furthermore, benefitting from an extraordinary working mechanism, the PTPA-CNBr device reveals a superb response-ability for the duration time of 0.1 ms (white light and blue light) as shown in Figure 5d,e, and the results of the real-time current and device monitoring images are also recorded and demonstrated in Video in the Supporting Information. Moreover,

we promote the scanning resolution utilizing the fastest sampling setup and the result is demonstrated in Figure S11 in the Supporting Information. It is worth noting that the interlayer exciton recombination could be generated rapidly under single-pulse stimulation as in the aforementioned pulse-PL experiment (Figure S7, Supporting Information). Namely, the AIE-polymer electret creating ultrafast interlayer recombination with the excitons from semiconductor for the photonic memory possesses the potential to realize photoprogramming operation within 60 ps of exposure time.

To investigate the effect of voltage-driven erasing capabilities for the photoinduced memory devices, a flow diagram of four successive steps was designed to read out the value of I_{DS} dependent on the modulated gate-voltage as summarized in the upper graphs of Figure 5f,g: (1) positive gate voltage (50 V) was repeated 3 times for the electrical-programming procedure; (2) one blue light pulse for 5 and 1 s (PTPA-CN and PTPA-CNBr) acts as the beginning photoprogramming step; (3) negative gate voltage (-50 V) was applied repeatedly 20 times for the electrical-erasing procedure; and (4) the value of I_{DS} in the final state was read for the PTPA-CN/PTPA-CNBr devices at a gate voltage of 20/15 V, respectively. To monitor the responding current in steps 1–3, the off-state reading mode was embedded between each disposed of step, as shown in the bottom graphs of Figure 5f,g. In the first step, the electrical-programming process could not successfully achieve the trapping-electron behavior by external positive electrical bias that could ensure the conductive current remaining in off-state before illumination. In step 2, After injecting photons into memory devices, the photogenerated electrons could reside in the electret layer, and the relevant current instantly

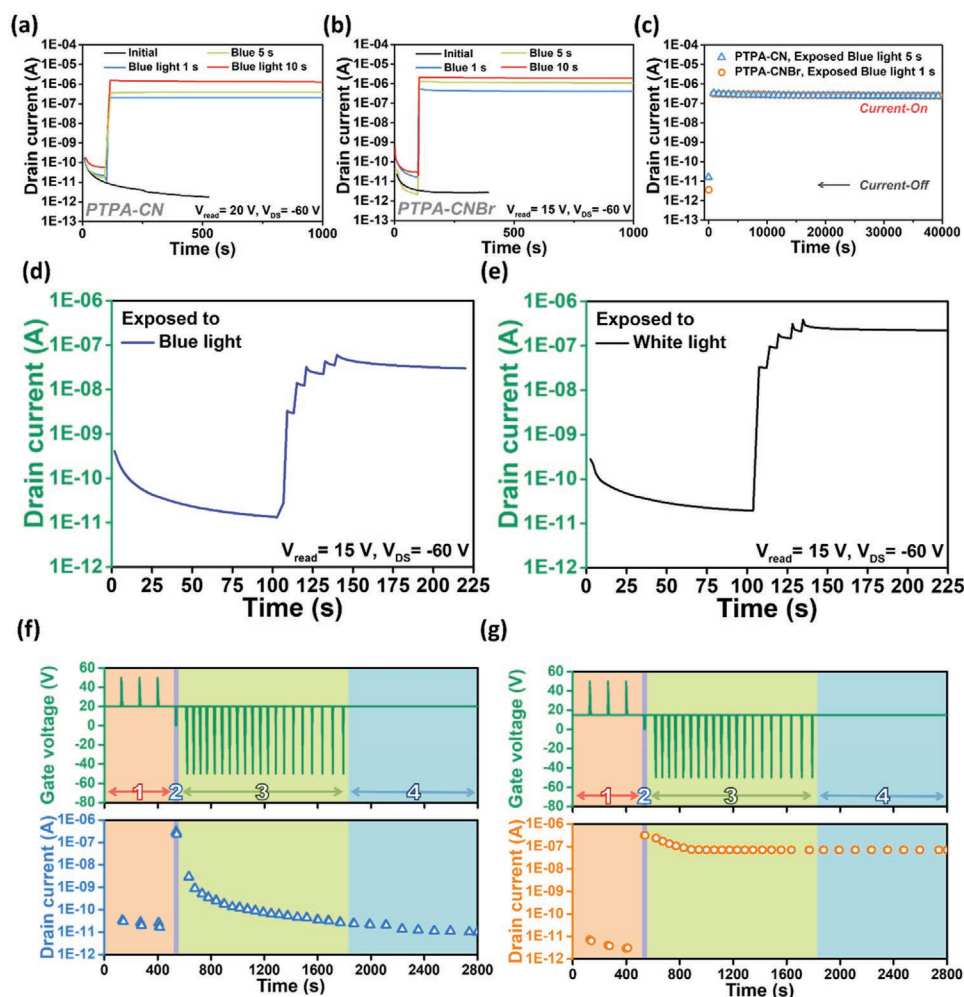


Figure 5. Transient characteristic of the photonic transistor memory based on a) PTPA-CN, b) PTPA-CNBr at $V_{DS} = -60$ V and $V_{read} = 20/15$ V by using light stimulation with a fixed wavelength of 405 nm, and exposure time varied from 1 to 10 s. c). Long-term stability of the readout current for the PTPA-CN and PTPA-CNBr device. The multilevel behavior of the PTPA-CNBr photonic memory at $V_{DS} = -60$ V with an illuminating time of 0.1 ms under d) blue and e) white flashlight for 5 times. Continuous gate-bias stresses on the device with f) PTPA-CN and g) PTPA-CNBr electret. Step 1: electric-programming pulse with +50 V, repeated three times, Step 2: photoprogramming pulse under blue light 5/1 s, performed once, Step 3: electrical-erasing pulse with -50 V, repeated 20 times, Step 4: reading at a gate bias of 20/15 V, $V_{DS} = -60$ V.

turns into on-state with a recognizable high current of 10^{-6} A. Afterward, the programmed devices with trapped electrons in the electret layer were attempted for recovery to the initial state through applying continuous 20 times negative gate pulses. By extending the read-out current time, it could be confirmed that the programmed PTPA-CN device could be reliably restored to the initial state in step 3. However, the PTPA-CNBr could still preserve most of the electrons in the electret layer for the read-out I_{DS} of marginally decreasing as shown in region 3 of Figure 5g. The I_{DS} in PTPA-CNBr devices maintains at 10^{-7} A over 1000 s without pronounced decay and displays a distinctly on/off current ratio of 10^5 even by utilizing compact electrical stress operation. These results manifest that the transistor memory devices employing PTPA-CN and PTPA-CNBr as charge storage materials exhibit exceptional nonvolatile flash and WORM-type memory performance, respectively. That is, the tunable memory behavior could be achieved by twisting the dihedral angle between donor and acceptor moieties as

illustrated in Figure S12 in the Supporting Information. In the nutshell, to correspond with the requirements of different communication devices, the versatile memory behaviors can be accomplished through molecular design strategies.

3. Conclusion

In conclusion, we have successfully developed an authentic nonvolatile photonic transistor memory device based on AIE-polymer electrets for the first time. Herein, the proposed mechanism of photoinduced programming for memory devices using AIE-active polymers as electrets has been comprehensively elucidated. This photoprogramming behavior was realized by constituting the appropriate energy level between semiconductor and electret layer and creating the situation of dual-layer excitation. Then, the interlayer excitons formed spontaneously could be directly observed by the optical analyses. Furthermore,

the semiconductor absorbs the light emitted from the AIE-polymers efficiently to generate numerous additional excitons, resulting in a significant enhancement of the memory-window behavior. Through integrating applied electrical-field and light-stimulation (in situ), the superior memory characteristics could be accomplished readily under ultrafast programming time of 0.1 ms, including a high current switch ratio up to 10^6 and a long retention time over 40 000 s. Besides, we propose the coherence between the charge storage behaviors and molecular design strategy, which provides the potential for versatile applications in future light-communication technology.

Supporting Information

Supporting Information is available from the Wiley Online Library or from the author.

Acknowledgements

G.-S.L. and Y.-C.C. received financial support from “Advanced Research Center for Green Materials Science and Technology” from The Featured Area Research Center Program within the framework of the Higher Education Sprout Project by the Ministry of Education in Taiwan (109L9006). M.-N.C., Y.-T.L., Y.-C.C., C.-Y.K., M.-H.C., and G.-S.L., received financial support from the Ministry of Science and Technology in Taiwan (MOST 109-2634-F-002-042, 109-2221-E-011-150, 107-2113-M-002-024-MY3, 107-2221-E-002-066-MY3). Besides, the authors also thank Dr. Bi-Hsuan Lin at the National Synchrotron Radiation Research Center, Hsinchu, Taiwan for the helpful advice on pulse-PL measurements.

Conflict of Interest

The authors declare no conflict of interest.

Data Availability Statement

Research data are not shared.

Keywords

AIE polymers, interlayer exciton, photonic transistor memory, polymer electrets, pulse PL

Received: February 5, 2021

Revised: April 2, 2021

Published online: April 28, 2021

[1] a) Q. Cheng, M. Bahadori, M. Glick, S. Rumley, K. Bergman, *Optica* **2018**, *5*, 1354; b) H. Haas, *Rev. Phys.* **2018**, *3*, 26.

- [2] a) G. W. Burr, R. M. Shelby, A. Sebastian, S. Kim, S. Kim, S. Sidler, K. Virwani, M. Ishii, P. Narayanan, A. Fumarola, *Adv. Phys. X* **2017**, *2*, 89; b) N. K. Upadhyay, H. Jiang, Z. Wang, S. Asapu, Q. Xia, J. J. Yang, *Adv. Mater. Technol.* **2019**, *4*, 1800589; c) Y. van De Burgt, A. Melianas, S. T. Keene, G. Malliaras, A. Salleo, *Nat. Electron.* **2018**, *1*, 386.
- [3] Y. Zhou, S. T. Han, X. Chen, F. Wang, Y. B. Tang, V. Roy, *Nat. Commun.* **2014**, *5*, 4720.
- [4] a) Y. Zang, H. Shen, D. Huang, C. A. Di, D. Zhu, *Adv. Mater.* **2017**, *29*, 1606088; b) L. Zhang, T. Wu, Y. Guo, Y. Zhao, X. Sun, Y. Wen, G. Yu, Y. Liu, *Sci. Rep.* **2013**, *3*, 1080.
- [5] K. Ishimaru, 2019 IEEE International Electron Devices Meeting (IEDM), San Francisco, December **2019**.
- [6] a) X. Tian, W. Xue, B. Zhang, X. Xu, Y. Chen, G. Liu, in *Photo-Electro-active Nonvolatile Memories for Data Storage and Neuromorphic Computing* (Eds: S. T. Han, Y. Zhou), Elsevier, Amsterdam, Netherlands **2020**, p. 223; b) Y. Yu, Q. Ma, H. Ling, W. Li, R. Ju, L. Bian, N. Shi, Y. Qian, M. Yi, L. Xie, *Adv. Funct. Mater.* **2019**, *29*, 1904602.
- [7] a) S. Lan, J. Zhong, E. Li, Y. Yan, X. Wu, Q. Chen, W. Lin, H. Chen, T. Guo, *ACS Appl. Mater. Interfaces* **2020**, *12*, 31716; b) R. C. Shallcross, P. Zacharias, A. Köhnen, P. O. Körner, E. Maibach, K. Meerholz, *Adv. Mater.* **2013**, *25*, 469; c) H. Yang, Y. Yan, X. Wu, Y. Liu, Q. Chen, G. Zhang, S. Chen, H. Chen, T. Guo, *J. Mater. Chem. C* **2020**, *8*, 2861.
- [8] a) J. Y. Chen, Y. C. Chiu, Y. T. Li, C. C. Chueh, W. C. Chen, *Adv. Mater.* **2017**, *29*, 1702217; b) Y. Qiao, Y. Lin, S. Zhang, J. Huang, *Chem. - Eur. J.* **2011**, *17*, 5180; c) C. C. Shih, Y. C. Chiang, H. C. Hsieh, Y. C. Lin, W. C. Chen, *ACS Appl. Mater. Interfaces* **2019**, *11*, 42429.
- [9] a) A. W. Hains, Z. Liang, M. A. Woodhouse, B. A. Gregg, *Chem. Rev.* **2010**, *110*, 6689; b) O. Ostroverkhova, *Chem. Rev.* **2016**, *116*, 13279.
- [10] Y. H. Chang, C. W. Ku, Y. H. Zhang, H. C. Wang, J. Y. Chen, *Adv. Funct. Mater.* **2020**, *30*, 2000764.
- [11] C. Y. Ke, M. N. Chen, Y. C. Chiu, G. S. Liou, *Adv. Electron. Mater.* **2021**, *7*, 2001076.
- [12] a) R. Hu, A. Qin, B. Z. Tang, *Prog. Polym. Sci.* **2020**, *100*, 101176; b) J. Li, J. Wang, H. Li, N. Song, D. Wang, B. Z. Tang, *Chem. Soc. Rev.* **2020**, *49*, 1144.
- [13] a) K. J. Baeg, Y. Y. Noh, J. Ghim, S. J. Kang, H. Lee, D. Y. Kim, *Adv. Mater.* **2006**, *18*, 3179; b) H. Klauk, M. Halik, U. Zschieschang, G. Schmid, W. Radlik, W. Weber, *J. Appl. Phys.* **2002**, *92*, 5259.
- [14] a) P. Cudazzo, M. Gatti, A. Rubio, *Phys. Rev. B* **2012**, *86*, 195307; b) J. Lee, S. Kim, K. Kim, J. H. Kim, S. Im, *Appl. Phys. Lett.* **2004**, *84*, 1701.
- [15] a) H. Chen, X. Wen, J. Zhang, T. Wu, Y. Gong, X. Zhang, J. Yuan, C. Yi, J. Lou, P. M. Ajayan, *Nat. Commun.* **2016**, *7*, 12512; b) P. Rivera, J. R. Schaibley, A. M. Jones, J. S. Ross, S. Wu, G. Aivazian, P. Klement, K. Seyler, G. Clark, N. J. Ghimire, *Nat. Commun.* **2015**, *6*, 6242; c) T. Zhu, L. Yuan, Y. Zhao, M. Zhou, Y. Wan, J. Mei, L. Huang, *Sci. Adv.* **2018**, *4*, eaao3104.
- [16] a) H. S. Lee, K. H. Lee, C. H. Park, P. J. Jeon, K. Choi, D.-H. Kim, H. R. Kim, G. H. Lee, J. H. Kim, S. Im, *J. Mater. Chem.* **2012**, *22*, 4444; b) L. Zhang, A. Sharma, Y. Zhu, Y. Zhang, B. Wang, M. Dong, H. T. Nguyen, Z. Wang, B. Wen, Y. Cao, *Adv. Mater.* **2018**, *30*, 1803986.
- [17] S. R. Forrest, *Philos. Trans. R. Soc., A* **2015**, *373*, 20140320.
- [18] M. Debucquoy, M. Rockelé, J. Genoe, G. Gelinck, P. Heremans, *Org. Electron.* **2009**, *10*, 1252.
- [19] a) Y. C. Chiu, H. S. Sun, W. Y. Lee, S. Halila, R. Borsali, W. C. Chen, *Adv. Mater.* **2015**, *27*, 6257; b) G. Zhang, Y. J. Lee, P. Gautam, C. C. Lin, C. L. Liu, J. M. W. Chan, *J. Mater. Chem. C* **2019**, *7*, 7865.